Available online at www.sciencedirect.com
ScienceDirect
Journal of the European Ceramic Society 27 (2007) 3069–3073
www.elsevier.com/locate/jeurceramsoc

Milling effect on the microwave properties of $Ba_2Ti_9O_{20}$ investigated by EMP technique

Yi-Chun Chen [a,*], Tsung-Hsuan Hong [a], Hsiu-Fung Cheng [b], Chi-Ben Chang [c], Keh-Chyang Leou [c], I.-Nan Lin [d]

[a] *Department of Physics, National Cheng Kung University, Tainan 701, Taiwan, ROC*
[b] *Department of Physics, National Taiwan Normal University, Taipei 116, Taiwan, ROC*
[c] *Department of System and Engineering Science, National Tsing-Hua University, Hsinchu, Taiwan 300, ROC*
[d] *Department of Physics, Tamkang University, Tamsui 251, Taiwan, ROC*

Available online 18 January 2007

Abstract

The effects of milling process on the microstructure and microwave properties of $Ba_2Ti_9O_{20}$ materials were systematically investigated by the evanescent microwave probe (EMP) technique. It was found that although the reaction kinetics of $Ba_2Ti_9O_{20}$ materials was markedly enhanced by the high-energy-milling (HeM) process, the quality factor of the materials decreases with the duration in HeM process. SiO_2-contamination due to the HeM milling process (with Si_3N_4 media) is presumed to be the main cause. In this study, SiO_2-doped $Ba_2Ti_9O_{20}$ sample was adopted to enhance and trace the SiO_2 effect during HeM process. The EMP investigation on the microwave dielectric properties of the local region for the $Ba_2Ti_9O_{20}$ samples indicates that lossy Si/Ti-containing phases were expelled by the $Ba_2Ti_9O_{20}$ grains, which is especially obvious in the as-sintered sample surface. Si-contamination induced the abnormal grain growth phenomenon, which, in turn, degrades the microwave dielectric quality factor of the $Ba_2Ti_9O_{20}$ materials.

Keywords: Milling; Dielectric properties; $BaO–TiO_2$; Evanescent microwave microscopy

1. Introduction

$Ba_2Ti_9O_{20}$ phase in the $BaO–TiO_2$ system[1] has drawn a lot of interest because of its marvelous microwave dielectric properties, including high dielectric constant (K) and large quality factor ($Q \times f$).[2] However, it is difficult to prepare $Ba_2Ti_9O_{20}$ materials with consistent properties, since the intermediate phases, such as $BaTi_4O_9$ or $BaTi_5O_{11}$, are usually formed preferentially during the calcinations of the $BaCO_3–TiO_2$ mixture.[3] Therefore, even though the investigations on modification of $Ba_2Ti_9O_{20}$ materials via dopants[4–6] were widely performed, the results are still quite controversial. In this study, we utilized nano-sized $BaTiO_3$ and TiO_2 as starting materials to provide better homogeneity and higher activity for nucleation, and thus improved the reliability for fabricating $Ba_2Ti_9O_{20}$ materials. In addition to the traditional ball-milling (BM) process, the calcined powders were pulverized by the high-energy-milling (HeM) techniques to enhance the processing efficiency. The effect of SiO_2-contamination induced in the milling process is investigated. Moreover, to directly examine the connection between the dielectric properties and the microstructure of $Ba_2Ti_9O_{20}$ ceramics, we use the evanescent microwave probe (EMP) technique[7–9] to locally image the microwave response.

2. Experimental methods

$Ba_2Ti_9O_{20}$ samples were prepared by mixed oxide process. To improve nucleation activity, nano-sized $BaTiO_3$ powders (50 nm) were mixed with nano-sized TiO_2 powders (~40 nm) in a nominal composition of $Ba_2Ti_9O_{20}$. The mixtures were calcined at 1000 °C for 4 h in air, followed by pulverization, granulation, pelletazation process and then sintered at 1250–1350 °C for 4 h in air. High-energy-milling and ball-milling process were used for pulverizing the calcined powders. The high-energy-milled powders were further ball-milled for a very short period to disintegrate the soft agglomerates resulted in HeM process. The crystal structure and microstructure of the sintered samples were examined using X-ray diffraction

* Corresponding author. Tel.: +886 6275757565263; fax: +886 62747995.
E-mail address: ycchen93@mail.ncku.edu.tw (Y.-C. Chen).

0955-2219/$ – see front matter © 2006 Elsevier Ltd. All rights reserved.
doi:10.1016/j.jeurceramsoc.2006.11.070

and scanning electron microscopy. The density of the sintered materials was measured using Archimedes method. The microwave dielectric constant (K) and quality factor ($Q \times f$) of the $Ba_2Ti_9O_{20}$ samples were measured using a cavity method at 7–8 GHz.

An evanescent microwave probe was used to make non-destructive measurements of the dielectric properties for the samples. No metal contact layer is needed as electrode. The decaying wave with spatial frequency components higher than $1/\lambda$ was introduced to the sample through a sharpened metal tip. The tip radius R_0 was about 30 μm and mounted on the center conductor of a high-Q, $\lambda/4$ coaxial resonator. The resonator acted as both an electromagnetic field emitter and a detector. While scanning at regions with different microwave properties by direct contact mode, the probe detected the variations and perturbed the resonance state of the resonator. From the perturbation theory, we can perform quantitative analysis of the EMP measurement. The shift of the resonant frequency (Δf) and Q-value ($\Delta 1/Q$) of the EMP resonator are related to the dielectric properties of the local detecting region by the following equations[10]:

$$\frac{\Delta f}{f_0} = -\frac{\int_v(\Delta\varepsilon E_1E_0 + \Delta\mu H_1H_0)\,dv}{\int_v(\varepsilon_0 E_0^2 + \mu_0 H_0^2)\,dv} = A\left[\frac{\ln(1-b)}{b} + 1\right] \quad (1)$$

$$\Delta\left(\frac{1}{Q}\right) = -\frac{\int_v(\Delta\varepsilon'' E_1E_0 + \Delta\mu'' H_1H_0)\,dv}{\int_v(\varepsilon_0 E_0^2 + \mu_0 H_0^2)\,dv} = -\left(\frac{1}{Q_0} + 2\tan\delta\right)\frac{\Delta f}{f_0} \quad (2)$$

where $\Delta f = f_r - f_0$, $\Delta(1/Q) = 1/Q - 1/Q_0$. f_0 and Q_0 are the original resonant frequency and quality factor, respectively, while f_r and Q_r are the measured resonant frequency and quality factor with a sample placed in adjacent to the EMP probe. $b = K - 1/K + 1$, where K is the dielectric constant of the sample. A is a constant determined by the geometry of the tip-cavity assembly which should be calibrated using standard samples (MgO, $K \sim 10$). In our system, the EMP resonator-tip system has the original resonant frequency $f_0 \sim 2665.5$ MHz and the quality factor $Q_0 \sim 820$. The calibrated parameter A is about 0.0033. Due to the local intense field distribution caused by tip-probe, high spatial resolution and high sensitivity can be obtained.

3. Results and discussion

With nano-sized powders as starting materials, the transformation kinetics for $Ba_2Ti_9O_{20}$ phase was highly improved. Fig. 1(a) shows that for the samples prepared by the BM-process, pure $Ba_2Ti_9O_{20}$ Hollandite-like phase can be easily obtained after sintering. The densities of thus obtained materials, which increase monotonously with the sintering temperature, achieved about 98.3% theoretical density (T.D.) when the samples are sintered at 1350 °C (Table 1). In spite that the BM-process can prepare $Ba_2Ti_9O_{20}$ materials with good stability, it takes too much time (>16 h) to disintegrate the calcined powders into sub-micron size. A new pulverization technique, the high-energy-milling process, which possesses overwhelmingly better milling efficiency to pulverize the calcined powders, is thus adopted. As illustrated in Fig. 1(b), the calcined powders followed by only 0.25 h HeM process can be fully converted to Hollandite-like structure after sintered at 1350 °C. Table 1 shows that a density higher then 96% T.D. was obtained for samples processed by 0.5 h HeM using Si_3N_4 grinding media (Si_3N_4-HeM). However, unlike the BM processed samples, the Si_3N_4-HeM processed samples behave abnormally, i.e., their densities and microwave dielectric properties decrease with the milling time. Meanwhile, the quality factor for the HeM processed materials is markedly inferior to the BM-processed ones.

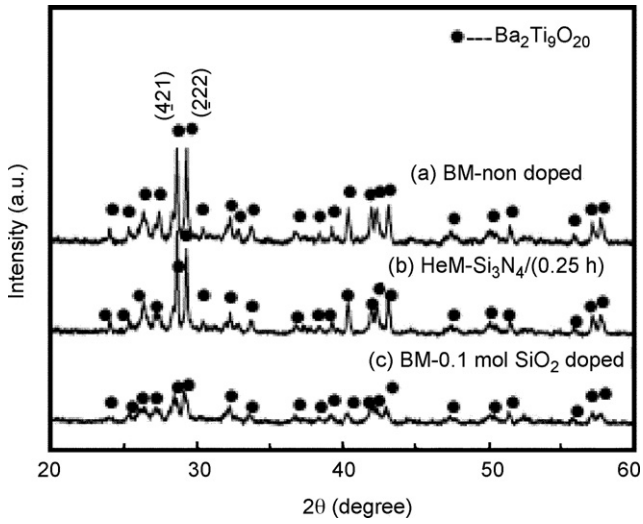

Fig. 1. X-ray diffraction patterns of the $Ba_2Ti_9O_{20}$ materials. The prepared powers are (a) ball-milled and non-doped, (b) high-energy milled by Si_3N_4 grinding ball and (c) ball-milled and 0.1 mol.%SiO_2-doped.

The possible explanation to degrade the HeM processed samples is the SiO_2-contamination induced by the milling process with Si_3N_4 jar and grinding balls. The EDAX analyses in SEM indicate that the average Si-content is higher for the samples processed for longer periods. To investigate how the Si-contamination affects the microwave dielectric properties of the $Ba_2Ti_9O_{20}$ materials, 0.1 mol.% SiO_2 was incorporated into the raw materials to amplify and trace the mechanism. Fig. 1(c) shows that although the SiO_2-doped BM materials are of pure Hollandite-like phase, the addition of SiO_2 significantly lowers the sharpness of the diffraction peaks, which implies the existence of incompletely transformed phase. Table 1 reveals that the density of the SiO_2-doped BM samples decreases markedly and

Table 1
Variation of the characteristics of the $Ba_2Ti_9O_{20}$ materials with the milling process

Milling process	Density (% of T. D.)	Dielectric constant	Quality factor $Q \times f$ (GHz)
Ball mill (non doped)	98.3	39.0	26,500
High energy mill (Si_3N_4 media)	97.5	38.4	21,900
Ball mill (SiO_2 doped)	92.8	35.3	14,600

is only about 92.8% T.D. for the 1350 °C-sintered $Ba_2Ti_9O_{20}$ materials. Table 1 also shows similar degrading tendency of microwave properties for the HeM processed and SiO_2-doped materials. The K-value of the materials correlates intimately with the sintered density, regardless whether they are SiO_2-doped or undoped, while the $Q \times f$-value of HeM and SiO_2-doped samples decreases significantly with the possible ratio of SiO_2-content.

Since the SiO_2 species cannot be clearly resolved by X-ray diffraction technique, the evanescent microwave probe technique incorporated with SEM study is utilized to provide more direct evidence. In contrast to the uniform grains of the BM samples, Fig. 2(a) shows that on the as-sintered surface of SiO_2-doped samples, large grains about several tens of microns in length are observed, coexisting with the small grains about few square micrometer in size. Moreover, EDAX in SEM analysis reveals that the SiO_2 species incorporated in the samples are mainly accumulated in the fine grain region, but the interior of the large grains is essentially free of the SiO_2. The dielectric images scanned by EMP (Fig. 2(b and c)) show similar distributions as the SEM image. The high frequency regions ($f_r \sim 2655$ MHz) in EMP frequency mapping (Fig. 2(b)) possess lower dielectric constant because of the smaller capacitance between the tip and sample local area. From the quantitative analysis of Eq. (1), the K values in these regions are about 8.0, which strongly implies the rich contamination of SiO_2 ($K \sim 4.0$). By contrast, most high-K regions in Fig. 2(b) with resonant frequency $f_r \sim 2648$ MHz are of dielectric constant $K \sim 34$, which is a little lower than those for the typical $Ba_2Ti_9O_{20}$ phases ($K \sim 39.9$) and may come from the small amount of incompletely transformed phases, such as $BaTi_4O_9$ or even amorphous phase.

Fig. 2(c) reveals the EMP Q-value image on the as-sintered surface of the SiO_2-doped $Ba_2Ti_9O_{20}$ sample. It should be noted that the absolute Q-value in Fig. 2(c) is the quality factor of the resonator perturbed by the tangent loss of the sample, as shown in Eq. (2), not for the sample itself. However, the Q-mapping still illustrates the relative quality factor distribution. Fig. 2(c) shows good relations with Fig. 2(b) and SEM microstructures. In Fig. 2(b), the low-K (high f_r) regions are composed by small clusters, which corresponds to the aggregations of the fine SiO_2-rich grains in SEM images, while the high-K (low f_r) regions are widely spread for a large area, as the abnormal large grains in Fig. 2(a). Fig. 2(c) indicates that the low-K, SiO_2-rich clusters also posses low quality factor, whereas the high K, SiO_2-free areas posses high Q-value. These results imply that the SiO_2-species are basically non-dissolvable in $Ba_2Ti_9O_{20}$ lattices, i.e., the SiO_2 species will be expelled by the $Ba_2Ti_9O_{20}$ grains and mostly precipitated at the sample surface.

EMP examinations were also taken in the interior of the samples by scanning the further polished surface where the as-sintered exterior was removed. Fig. 3(a) reveals that for the BM $Ba_2Ti_9O_{20}$ samples, the aggregated clusters are about the same size and the distribution of microwave dielectric constant is quite uniform. The main matrices with K-value about 40 ($f_r \sim 2645.6$ MHz) imply that the BM samples are constituted by pure $Ba_2Ti_9O_{20}$ phases. As for the HeM samples (Fig. 3(b)),

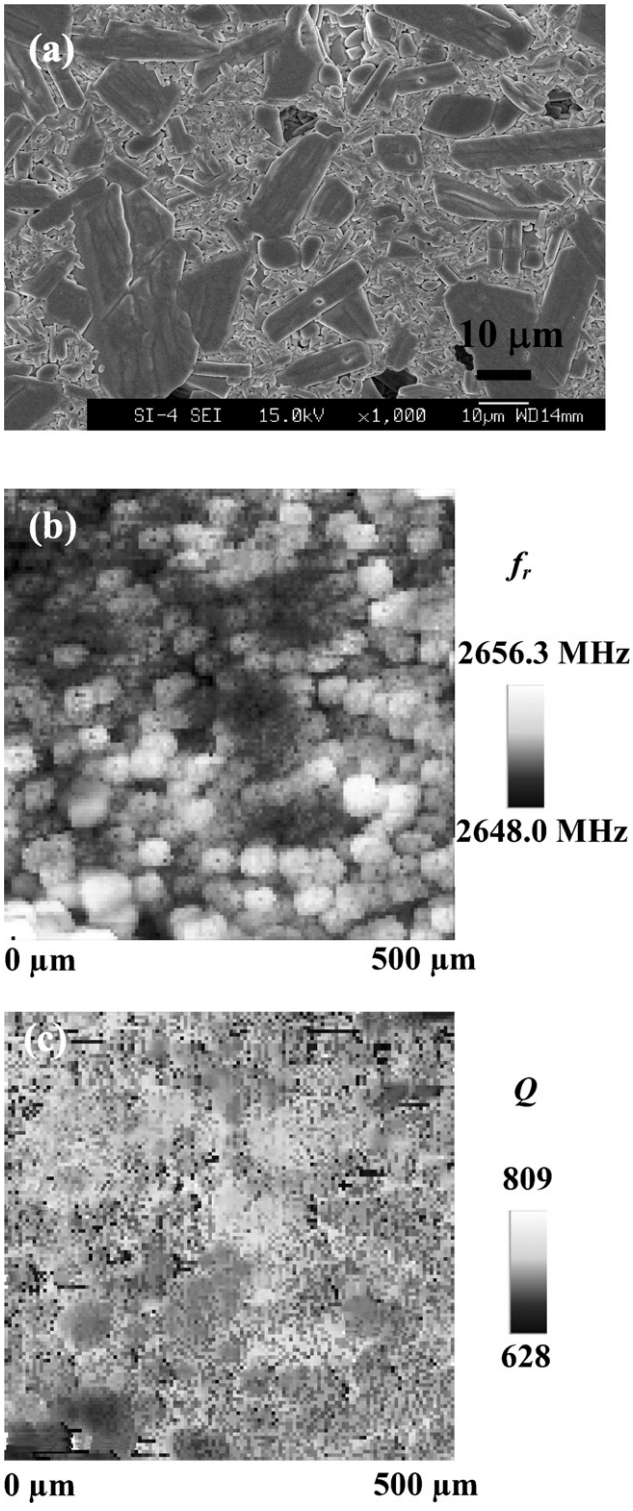

Fig. 2. (a) The SEM microstructure, (b) the EMP frequency image and (c) the EMP Q image on the as-sintered surface for the 0.1 mol.% SiO_2-doped $Ba_2Ti_9O_{20}$ materials. The samples were sintered at 1350 °C for 4 h.

most regions still possess dielectric constant about 40; however, compared with the surface of BM samples, the incompletely transformed phases ($f_r \sim 2647.5$ MHz, $K \sim 37$) increase markedly. Moreover, near the low-K region, a small amount of phases with high dielectric constant ($f_r \sim 2643.5$ MHz, $K \sim 60$)

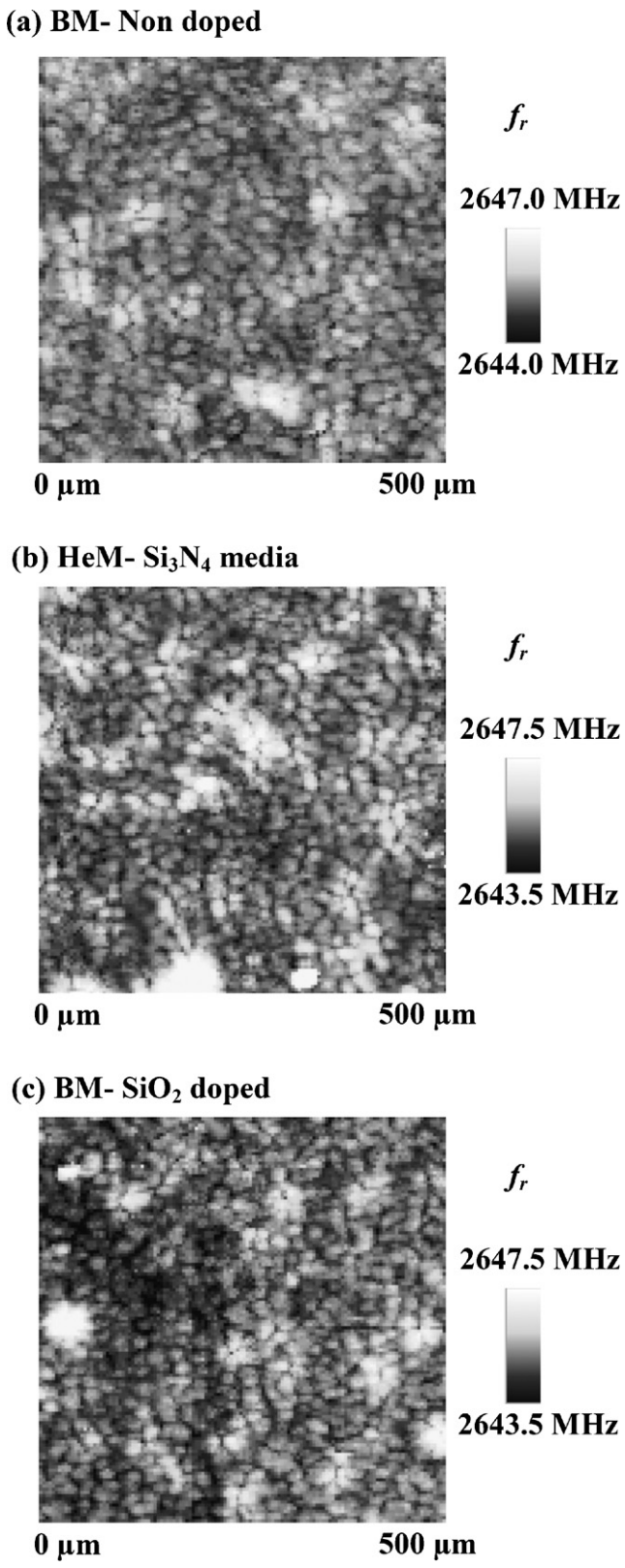

Fig. 3. EMP frequency images on polished surface for (a) ball-milled and non-doped, (b) high-energy milled and (c) ball-milled and 0.1 mol.% SiO_2-doped $Ba_2Ti_9O_{20}$ materials.

were observed. Almost certainly, these regions are contaminated by TiO_2, which has dielectric constant about 100. The proportion of extremely high-K clusters or low-K clusters expanded significantly in the SiO_2-doped BM samples (Fig. 3(c)). Again, the SiO_2-doped samples show similar but more intense behaviors in the tendency of degradation with the HeM ones, indicating that the deleterious effect from HeM process can be attributed to the SiO_2-contamination. In addition, unlike the as-sintered surface, Fig. 3(c) shows that the SiO_2-rich clusters ($K \sim 8$) almost disappeared in the interior of the SiO_2-doped samples. The EMP results in Figs. 2 and 3 imply that the SiO_2 species will interact with the $Ba_2Ti_9O_{20}$ materials, inducing the formation of the TiO_2 and $BaTi_4O_9$ secondary phases. The SiO_2 species will be mainly expelled to the sample surface, improving the formation of liquid phase during sintering, and then brings the abnormal grain growth. The SiO_2-rich or TiO_2-rich phases are the main causes to lower the quality factors of the HeM $Ba_2Ti_9O_{20}$ materials.

4. Conclusions

Evanescent microwave probe technique had been used to directly investigate the mechanism of the deterioration in quality factor during the high-energy-milling process. Presumably, the contamination of SiO_2, which comes from the Si_3N_4 grinding media in HeM process, is the main cause. The SiO_2-doped samples shows similar but more intense tendency of the property degradation with the HeM samples. EMP studies reveal that the additional SiO_2 species will induce abnormal grain growth, and results in the formation of TiO_2-rich and SiO_2-rich phases in the interior and exterior surface of the sample, respectively. The small amounts of low-quality phases cannot be observed by X-ray diffractions, but significantly degrade the $Ba_2Ti_9O_{20}$ samples.

Acknowledgements

Financial support of National Science Council, ROC through the project NSC 95-2112-M-006-003 and NSC 94-2112-M-032-005 are gratefully acknowledged by the authors.

References

1. Jonker, G. H. and Kwestroo, W., Ternary system BaO–TiO_2–SnO and BaO–TiO_2–ZrO_2. *J. Am. Ceram. Soc.*, 1958, **41**, 390–394.
2. O'Bryan, H. M., Thomson Jr., J. and Plourde, J. K., A new BaO–TiO_2 compound with temperature-stable high permittivity and low microwave loss. *J. Am. Ceram. Soc.*, 1974, **57**, 450–453.
3. Wu, J. M. and Wang, H. W., Factors affecting the formation $Ba_2Ti_9O_{20}$. *J. Am. Ceram. Soc.*, 1988, **71**, 869–875.
4. O'Bryan, H. M. and Thomson Jr., J., Phase Equilibrium in the TiO_2-rich region of the system BaO–TiO_2. *J. Am. Ceram. Soc.*, 1974, **57**, 522–526.
5. Lin, W. Y. and Speyer, R. F., Microwave properties of $Ba_2Ti_9O_{20}$ doped with zirconium and tin oxides. *J. Am. Ceram. Soc.*, 1999, **82**, 1207–1211.
6. Fallon, G. D. and Gatehouse, B. M., The crystal structure of $Ba_2Ti_9O_{20}$: a hollandite related compound. *J. Solid State Chem.*, 1983, **49**, 59–64.
7. Lu, Y., Wei, T., Duewer, F., Ming, N. B., Schultz, P. G. and Xiang, X. D., High spatial resolution quantitative microwave impedance microscopy

by a scanning tip microwave near-field microscope. *Science*, 1997, **276**, 2004–2006.

8. Chen, Y.-C., Cheng, H.-F., Wang, G., Xiang, X.-D., Chiang, Y.-C., Liu, K.-S. *et al.*, Microwave dielectric imaging of $Ba_2Ti_9O_{20}$ materials with a scanning-tip microwave near-field microscope. *J. Eur. Ceram. Soc.*, 2003, **23**, 2667–2670.
9. Chen, Y.-C., Yao, Y.-D., Hsieh, Y.-S., Cheng, H.-F., Chia, C.-T. and Lin, I.-N., Microwave dielectric mechanism studied by microwave near-filed microscopy and Raman spectroscopy. *J. Electroceram.*, 2004, **13**, 281–286.
10. Gao, C. and Xiang, X. D., Quantitative microwave near-field microscopy of dielectric properties. *Rev. Sci. Instrum.*, 1998, **69**, 3846–3851.